



# How does intestinal-type intraductal papillary mucinous neoplasm emerge? CDX2 plays a critical role in the process of intestinal differentiation and progression

Yuko Omori<sup>1</sup> · Yusuke Ono<sup>2,3</sup> · Toshikazu Kobayashi<sup>1,4</sup> · Fuyuhiko Motoi<sup>5</sup> · Hidenori Karasaki<sup>2</sup> · Yusuke Mizukami<sup>2,3</sup> · Naohiko Makino<sup>4</sup> · Yoshiyuki Ueno<sup>4</sup> · Michiaki Unno<sup>5</sup> · Toru Furukawa<sup>1</sup>

Received: 3 October 2019 / Revised: 2 March 2020 / Accepted: 25 March 2020 / Published online: 15 April 2020  
© Springer-Verlag GmbH Germany, part of Springer Nature 2020

## Abstract

Intestinal-type intraductal papillary mucinous neoplasm (IPMN) of the pancreas is clinicopathologically distinctive. Our research aimed to elucidate the molecular mechanism of the development and progression of the intestinal-type IPMN. In 60 intestinal-type IPMN specimens, histological transitions from gastric-type epithelia to intestinal-type epithelia were observed in 48 cases (80%). CDX2/MUC2/alcian blue triple staining indicated that CDX2 appeared to precede MUC2 expression and subsequent alcian blue-positive mucin production. Expression of p21 and Ki-67 seemed to be accelerated by CDX2 expression ( $p = 6.02e-13$  and  $p = 3.1e-09$ , respectively). p21/Ki-67 double staining revealed that p21 was mostly expressed in differentiated cells in the apex of papillae, while Ki-67 was expressed in proliferative cells in the base of papillae. This clear cellular arrangement seemed to break down with the progression of atypical grade and development of invasion ( $p = 0.00197$ ). Intestinal-type IPMNs harbored frequent *GNAS* mutations (100%, 25/25) and *RNF43* mutations (57%, 8/14) and shared identical *GNAS* and *KRAS* mutations with concurrent gastric-type IPMNs or incipient gastric-type neoplasia (100%, 25/25). *RNF43* mutations showed emerging or being selected in intestinal-type neoplasms along with  $\beta$ -catenin aberration. Activation of protein kinase A and extracellular-regulated kinase was observed in CDX2-positive intestinal-type neoplasm. These results suggest that gastric-type epithelia that acquire *GNAS* mutations together with induction of intrinsic CDX2 expression may evolve with clonal selection and additional molecular aberrations including *RNF43* and  $\beta$ -catenin into intestinal-type IPMNs, which may further progress with complex villous growth due to disoriented cell cycle regulation, acceleration of atypical grade, and advance to show an invasive phenotype.

**Keywords** Pancreatic cancer · Intraductal papillary mucinous neoplasm · *KRAS* · *GNAS* · *RNF43*

**Electronic supplementary material** The online version of this article (<https://doi.org/10.1007/s00428-020-02806-8>) contains supplementary material, which is available to authorized users.

✉ Toru Furukawa  
toru.furukawa@med.tohoku.ac.jp

<sup>1</sup> Department of Investigative Pathology, Tohoku University Graduate School of Medicine, 2-1, Seiryomachi, Aoba-Ku, Sendai 980-8575, Japan

<sup>2</sup> Institute of Biomedical Research, Sapporo Higashi Tokushukai Hospital, Sapporo 065-0033, Japan

<sup>3</sup> Department of Medicine, Asahikawa Medical University, Asahikawa 078-8510, Japan

<sup>4</sup> Department of Gastroenterology, Faculty of Medicine, Yamagata University, Yamagata 990-9585, Japan

<sup>5</sup> Department of Surgery, Tohoku University Graduate School of Medicine, Sendai 980-8574, Japan

## Introduction

Intraductal papillary mucinous neoplasms of the pancreas (IPMNs) include several distinct histopathological subtypes, namely, gastric, intestinal, pancreatobiliary, and oncocytic [1–3]. These subtypes are characterized by their morphologic features and the expression of distinct mucin proteins, which are known to be relevant to patient prognosis [4]. Intestinal-type IPMNs are characterized by intestinal-type papillae composed of tall columnar cells with cigar-shaped nuclei and abundant cytoplasm that is stained with alcian blue.

Cells of intestinal-type IPMNs specifically express mucin 2 (MUC2) in the cytoplasm [5, 6] and caudal-type homeobox 2 (CDX2) in nuclei [7]. MUC2 is a major gel-forming mucin encoded by the *MUC2* gene, and its expression is prominent

in the intestinal tract, where it is retained in apical cytoplasm and secreted into the lumen to serve as a mucosal protective barrier [5, 8]. CDX2 is encoded by the *CDX2* gene, one of the caudal-related homeobox transcription factor genes and is well known as a major regulator of intestine-specific gene expression associated with cell growth and differentiation [9, 10]. CDX2 interacts with the *MUC2* promoter and activates *MUC2* transcription in the differentiation of the goblet cells in the intestinal tract [11]. Simply put, CDX2 is the most likely candidate for a coordinator of the intestinal differentiation in IPMNs. The intestinal-type IPMNs are often concurrent with gastric-type IPMNs; therefore, the gastric-type IPMNs are assumed to be the origin of intestinal-type IPMNs. However, the mechanism of change of the epithelial type from gastric to intestinal, along with an apparent simultaneous increase of dysplastic grade from low to high, has not been explained.

In our study, we investigated the associations between intestinal-type IPMNs and concurrent gastric-type epithelia by means of detailed immunohistochemical examinations, including CDX2/MUC2/alcian blue triple staining and p21/Ki-67 double staining, and targeted amplicon sequencing in microdissected tissues for known driver genes for IPMNs, including *KRAS*, *GNAS*, *RNF43*, *CTNNB1*, *TP53*, *CDKN2A*, and *SMAD4* [12], and immunohistochemical analysis of  $\beta$ -catenin, p53, p16, and SMAD4 to elucidate the mechanism of the development and progression of intestinal-type IPMNs and to establish the molecular progression model.

## Methods

### Materials

Formalin-fixed and paraffin-embedded (FFPE) tissue samples of 60 consecutive intestinal-type IPMNs operated upon at the Tohoku University Hospital from January 2010 to January 2019 were obtained. Seventy-nine high-grade gastric, pancreatobiliary, and oncocytic-type IPMNs were also obtained for validation analysis. This study was approved by the Institutional Review Board of Tohoku University, Graduated School of Medicine (#2018-1-752).

### Histological evaluation

Intestinal-type IPMNs were characterized by villous papillae consisting of tall columnar cells with pseudostratified elongated nuclei and basophilic cytoplasm with variable amounts of apical mucin. The gastric-type neoplastic component was defined by low papillary to flat epithelium consisting of innocuous cells with basally oriented small round nuclei and abundant pale eosinophilic cytoplasm, reminiscent of the gastric foveolar epithelium (Fig. 1a–c). Pathological assessment of the subtypes and grades was conducted by two pathologists

(Y. Omori and T.F.) according to criteria described previously [1, 2, 13].

### Immunohistochemical analysis

Protein expression was examined by immunohistochemistry using the following antibodies on the 60 intestinal-type IPMNs: anti-CDX2 (DAK-CDX2, 1:50; DAKO/Agilent, Santa Clara, CA, USA), anti-MUC2 (CCP58, 1:200; Leica Biosystems, Nussloch, Germany), anti-MUC5AC (CLH2, 1:200; Leica Biosystems), anti-p21 (12D1, 1:100; Cell Signaling Technologies, Danvers, MA, USA), anti-Ki-67 (MIB-1, 1:100; DAKO/Agilent), anti-MutL Protein Homolog 1 (MLH1) (ES05, ready-to-use; DAKO/Agilent) as primary antibodies, and Histofine Simple Stain MAX-PO (Nichirei Biosciences, Tokyo, Japan) as a secondary antibody. Triple staining for CDX2, MUC2, and alcian blue was carried out on the 60 intestinal-type IPMNs and double immunostaining for p21 and Ki-67 was carried out on 43 intestinal-type IPMNs as described in the supplemental method. Protein expressions using the following antibodies: anti- $\beta$ -catenin (14, 1:500; BD Transduction Laboratories, Lexington, KY, USA), anti-p53 (DO-7, 1:100; DAKO/Agilent), anti-p16 (E6H4, ready-to-use; Roche, Heidelberg, Germany), and anti-Sma and Mad homolog 4 (SMAD4) (B-8, 1:100; Santa Cruz Biotech, Santa Cruz, CA, USA), anti-phospho-(Ser/Thr) cAMP-dependent protein kinase (PKA) substrate (#9621, 1:200; Cell Signaling Technologies), and anti-phospho-extracellular-regulated kinase 1/2 (ERK1/2) (D13.14.4E, 1:100; Cell Signaling Technologies) were assessed in 25 IPMNs subjected for mutation analysis.

Each CDX2 and MUC2 in a single immunostaining was quantitatively scored on the percentage of immunoreactivity in the neoplastic cells and classified as less than 5%, 5–50%, 51–90%, and more than 90%. Labeling indices of Ki-67 and p21 were counted manually. The distribution and association of the CDX2, MUC2, and alcian blue triad, and the p21 and Ki-67 dyad were analyzed in accordance with tumor grades and change in epithelial morphologic types. The nuclear and cytoplasmic stain of  $\beta$ -catenin, overexpression and complete loss of expression of p53, loss of expression of p16, loss and reduced expression of SMAD4, and loss of expression of MLH1 were assessed as aberrant. Histo-score of phospho-PKA substrate and labeling index of phospho-ERK1/2 was assessed in accordance with epithelial type.

### Mutation analysis

FFPE tissue samples were sectioned at 12- $\mu$ m thickness, and the intestinal-type and the gastric-type neoplastic components were separately microdissected with help of immunostaining (Supplementary Fig. S1). Neoplastic cellularity in each sample was estimated at more than 80%. Genomic DNA was

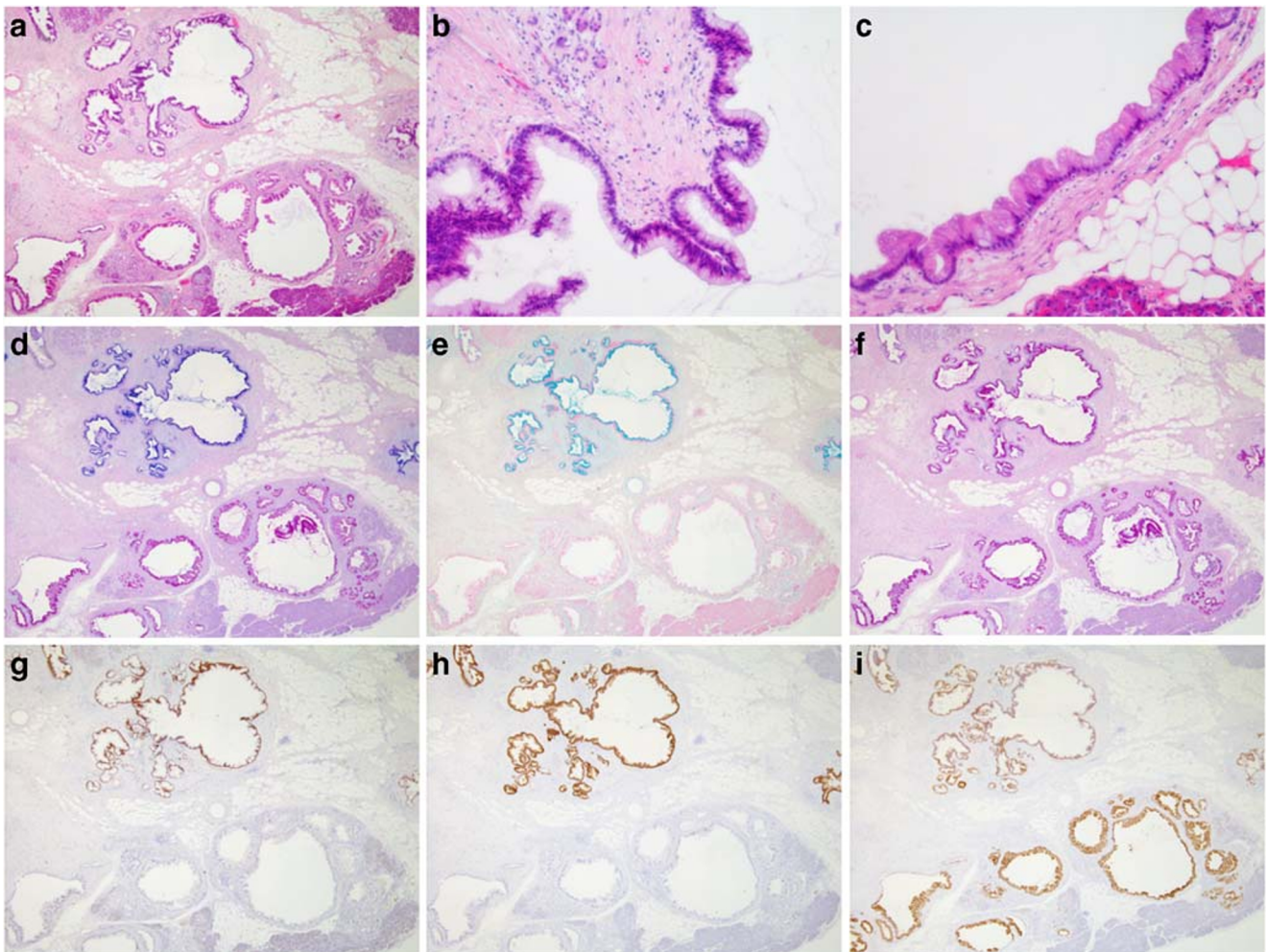


**Fig. 1** Mucins and CDX2 expression in intestinal-type intraductal papillary mucinous neoplasm. Intestinal-type intraductal papillary mucinous neoplasm (IPMN) concurrent with gastric-type component (a–c, hematoxylin and eosin staining, the intestinal-type component is shown in upper left of a and b, and the gastric-type component is shown in lower

part of a and c). Intestinal-type IPMNs had alcian blue-positive mucin (d, alcian blue and periodic acid-Schiff's stain, and e, alcian blue stain), while the entire IPMN had periodic acid-Schiff-positive mucin (f). Intestinal-type IPMNs expressed CDX2 (g) and MUC2 (h), while the entire IPMN expressed MUC5AC (i)

extracted using GeneRead DNA FFPE Kit (Qiagen, Hilden, Germany). Mutations in codons 12, 13, and 61 of *KRAS* and codon 201 of *GNAS* were analyzed in 25 IPMNs, of which 14 by targeted amplicon sequencing using Ion S5 System (Thermo Fisher Scientific, Waltham, MA, USA) and 11 using digital PCR (QX200 Droplet Digital PCR System; Bio-Rad, Hercules, CA, USA), as previously described [14]. Mutations of *RNF43*, *CTNNB1*, *TP53*, *CDKN2A*, and *SMAD4* were analyzed in 14 IPMNs by targeted amplicon sequencing using the custom panel covering the whole exon regions, as previously described [14].

### Statistical analysis

Categorical variables were assessed using Fisher's exact test. Continuous variables were assessed using the paired *t* test and one-way ANOVA. The correlation was evaluated by the

Pearson correlation coefficient. *p* values < 0.05 were considered statistically significant. Statistical analysis was performed using R (version 3.3.2; The R Foundation).

## Results

### Association of intestinal-type IPMNs and concurrent gastric-type neoplasms

We studied 60 cases of intestinal-type IPMNs, including those with low-grade dysplasia ( $n = 4$ ), high-grade dysplasia ( $n = 42$ ), and an associated invasive colloid carcinoma ( $n = 14$ ). Most of these intestinal-type IPMNs contained low-grade gastric-type neoplastic components.

Histologically, there were visible transitions from gastric-type neoplastic components to intestinal-type components in

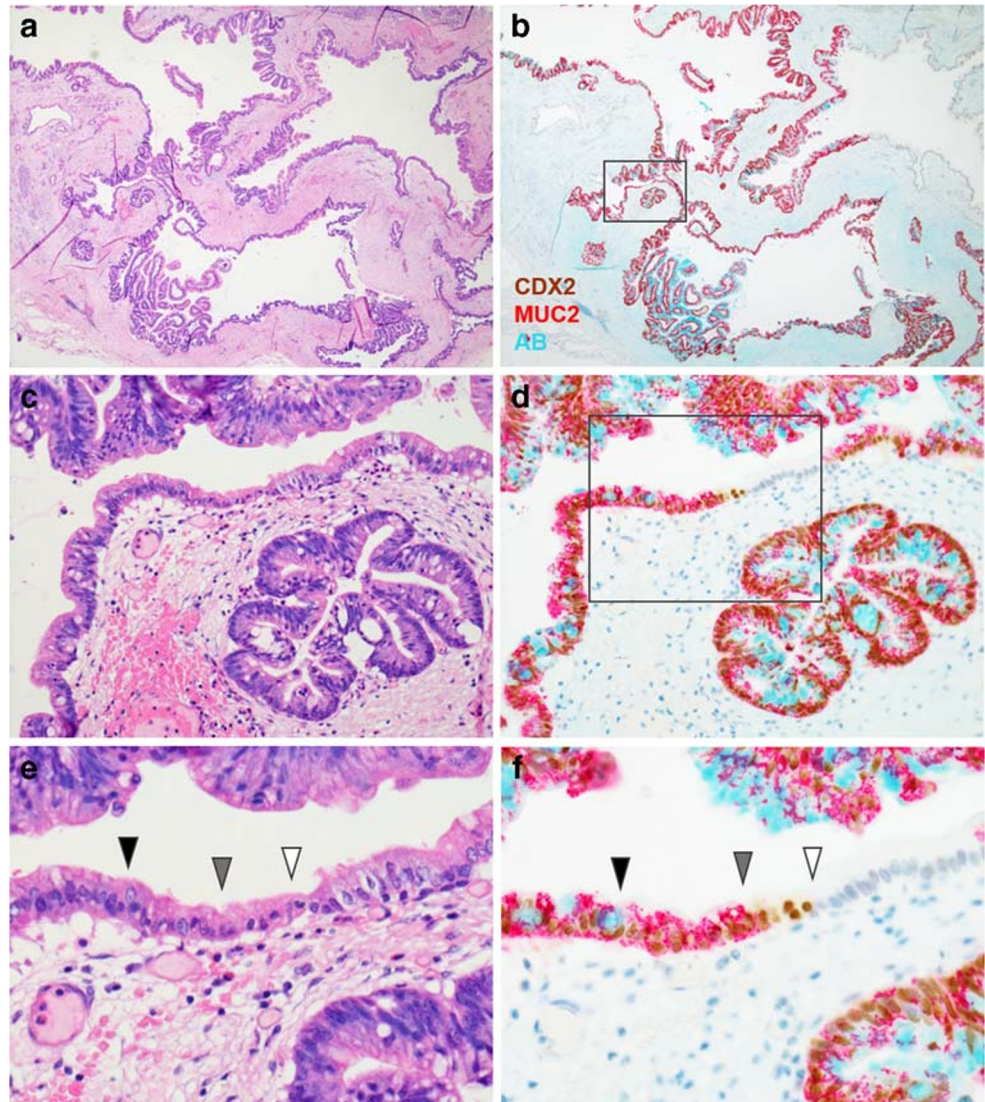
80% ( $n = 48$ ) of the examined cases (Fig. 2). During the transition, intestinal features appeared to emerge gradually in gastric-type neoplastic components of IPMNs ( $n = 30$ , 50.0%) or minute PanIN-like lesions ( $n = 18$ , 30.0%) (Supplementary Fig. S2). Goblet cell metaplasia was observed in concurrent gastric-type IPMNs prominently in 33.3% ( $n = 10$ ), slightly in 23.3% ( $n = 7$ ), and not at all in 44.3% ( $n = 13$ ). In contrast, the goblet cell metaplasia was rarely observed in concurrent minute PanIN-like lesions.

We evaluated the frequency of cells expressing CDX2, MUC2, and/or alcian blue-positive mucin. IPMNs basically express periodic acid-Schiff-positive mucin and MUC5AC, while typical intestinal-type IPMNs express alcian blue-positive cytoplasmic mucin, CDX2, and MUC2 (Fig. 1). In 95% ( $n = 57$ ), CDX2 expression was observed in over 90% of neoplastic cells, and the intensity and abundance of CDX2 expression were slightly higher than those of MUC2. The

amount of alcian blue-positive mucin production varied (Supplementary Fig. S3).

We performed triple staining for CDX2, MUC2, and alcian blue to visualize in detail the associations between those features so as to estimate the timing of the intestinal phenotype emergence (Supplementary Fig. S4). The results revealed that CDX2 expression appeared to precede MUC2 expression and morphological changes into intestinal-type neoplasms from gastric-type epithelia (Figs. 2 and 3). In detail, CDX2 expression was observed in gastric-type cuboidal cells with round nuclei without MUC2 expression (Figs. 2e, f and 3d, l). In adjacent cells showing features typical for morphological transition into intestinal-type cells, such as nuclear elongation, high-columnar epithelia, and nuclear stratification, MUC2 expression became obvious (Figs. 2e, f and 3e, m). In further continuous cells, cytoplasmic alcian blue-positive mucin and papillary growth seemed to become prominent as MUC2

**Fig. 2** Intestinal features emerged gradually in gastric-type IPMNs. HE staining (a, c, and e) and triple staining for CDX2 (nuclear brown staining), MUC2 (cytoplasmic red staining), and alcian blue (b, d, and f) of intestinal-type intraductal papillary mucinous neoplasm with gastric-type component. CDX2 appeared to express in gastric-type cuboidal epithelium with round nuclei (white arrow head) prior to MUC2 expression (gray arrow head, e and f). MUC2-positive neoplastic cells showed nuclear elongation, high-columnar epithelia, and nuclear stratification (gray arrowhead to black arrowhead, e and f). Cytoplasmic alcian blue-positive mucin and papillary growth became prominent as MUC2 expression increased (a–d)



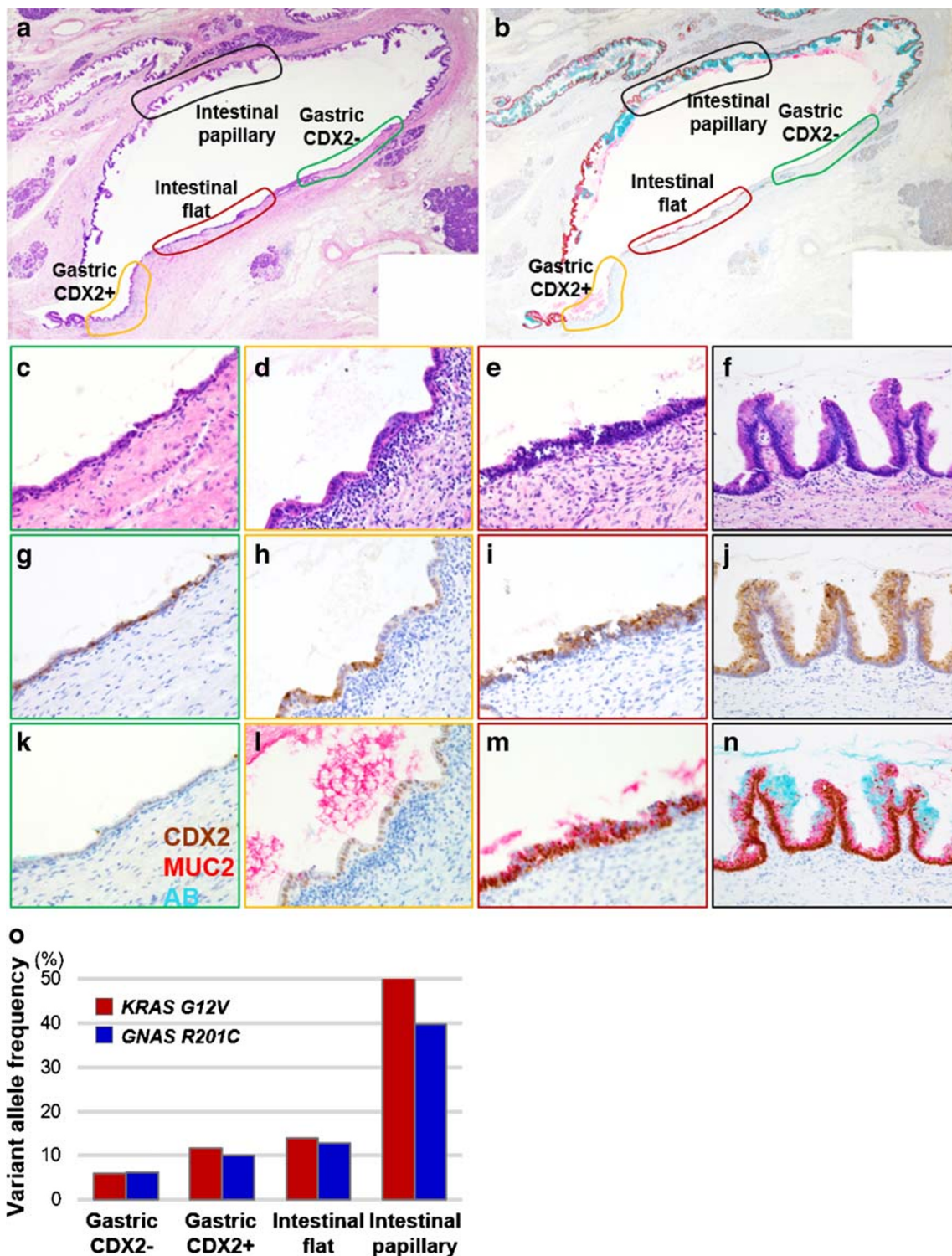


**Fig. 3** Intestinal features emerged gradually in PanIN-like gastric-type epithelium. HE staining (a, c–f), triple staining for CDX2 (nuclear brown staining), MUC2 (cytoplasmic red staining), and alcian blue (b, k–n), and MUC5AC immunostaining (g–j). CDX2 appeared to express in the gastric-type cuboidal epithelium with round nuclei (d, h, and l) without MUC2 expression (l). MUC2-positive neoplastic cells showed nuclear elongation, high-columnar epithelia, and nuclear stratification (e and

m). Cytoplasmic alcian blue-positive mucin and papillary growth become prominent as MUC2 expression increased (f and n). The results of mutation analysis on TU\_114\_IPMN are shown (o). *KRAS G12V* and *GNAS R201C* were detected in all stages of tumor development, from gastric-type PanIN-like lesions without CDX2 expression to intestinal-type IPMNs with papillary growth. The variant allele frequencies escalated with tumor maturation

expression increased (Fig. 2a–d and 3f, n). One or more transition sites were observed in the analyzed section. The transitions showed gastric-type epithelia in flat shape connected to intestinal-type epithelia in flat or low papillary shape, even in the case with marked papillary growth of intestinal neoplasm. In the case of an IPMN with prominent goblet metaplasia, the triple staining led to the same results: CDX2 expression appeared to precede MUC2 expression and the subsequent emergence of alcian blue-positive mucin (Supplementary Fig. S5).

### Expression patterns of p21 and Ki-67 in intestinal-type IPMNs

Next, we evaluated the associations of the expression of p21, a cell cycle arrest protein, and Ki-67, a cell proliferation marker, with the subtypes and neoplastic grades. Both seemed to be accelerated by CDX2 expression as follows (Fig. 4a, b, e, f): the labeling index of p21 was  $10.0 \pm 9.7\%$  in gastric-type IPMN components ( $n = 20$ ) and  $51.7 \pm 20.4\%$  in intestinal-type IPMN components ( $n = 54$ ,  $p = 6.02e-13$ ). The labeling index of Ki-67 was  $3.3 \pm 2.4\%$  in gastric-type IPMN components and  $29.5 \pm 17.2\%$  in intestinal-type IPMN components ( $p = 3.1e-09$ ). This phenomenon seemed specific for intestinal-type IPMNs, compared with IPMNs of high-grade gastric, oncocytic, and pancreatobiliary subtypes (Supplementary Fig. S6).

We performed double immunostaining for p21 and Ki-67 to visualize the associations of cells with those markers simultaneously and found that p21-positive cells tended to distribute in the apex, while Ki-67-positive cells did so in the base of papillae, which resembles their distribution in the normal intestinal mucosa (Fig. 4b, f, and inset). This organizational trend seemed to break down with the progression of grade and occurrence of invasion (Fig. 4c, d, g, h). p21 labeling indices of low-grade intestinal-type IPMNs ( $60.6 \pm 22.1\%$ ,  $n = 17$ ) were higher than those of high-grade IPMNs with a statistical trend ( $47.2 \pm 18.2\%$ ,  $n = 36$ ,  $p = 0.05002$ ) or those of invasive cancers with statistical significance ( $16.3 \pm 9.5\%$ ,  $n = 6$ ,  $p = 3.0e-06$ ). Moreover, Ki-67 labeling indices of low-grade intestinal IPMNs ( $13.6 \pm 9.4\%$ ) were lower than those of high-grade IPMNs with statistical significance ( $37.4 \pm 14.5\%$ ,  $p = 5.6e-09$ ). However, there was no statistical significance observed regarding the above in invasive cancers ( $25.0 \pm 17.6\%$ ,  $p = 0.262$ ). Labeling index of p21 tended to be higher than that of Ki-67 in intestinal-type IPMNs with low-grade dysplasia (Fig. 4f, j), but this trend was reversed with malignant progression to high-grade and invasive cancer (Fig. 4g–l). The Ki-67/p21 labeling index ratio increased with the malignant progression with statistical significance (Fig. 4i, low-grade intestinal IPMN,  $0.23 \pm 0.19$ , high-grade intestinal-type IPMN,  $1.13 \pm 1.07$ , invasive cancer,  $1.53 \pm 1.13$ , one-way ANOVA,  $p = 0.00197$ , paired  $t$  test, low-grade

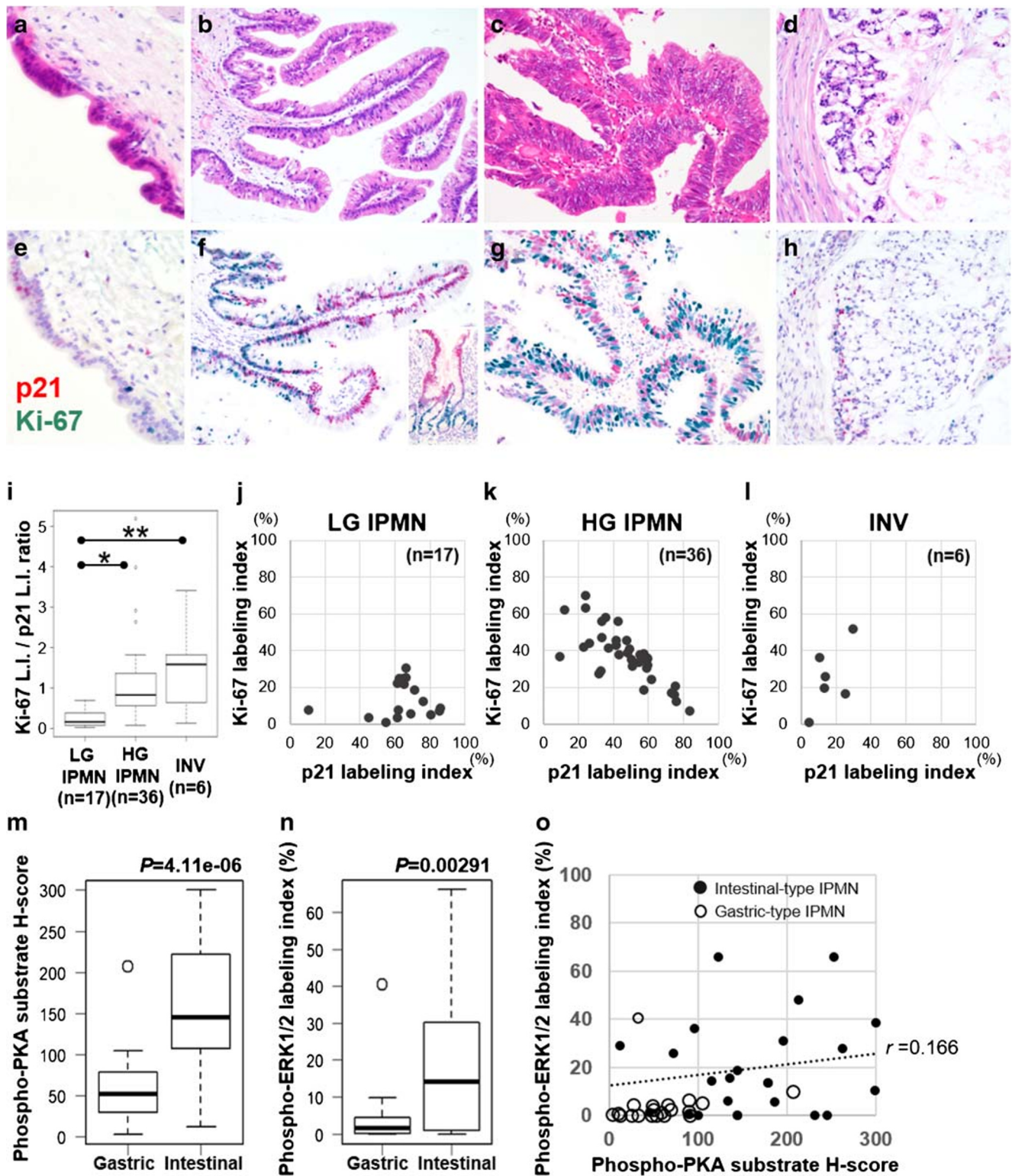
intestinal-type IPMN versus high-grade intestinal-type IPMN,  $p = 0.005$ , and versus invasive cancer,  $p = 0.013$ ).

### Mutation analysis of KRAS and GNAS in intestinal-type IPMNs

We further examined the mutations of *KRAS* and *GNAS* in microdissected neoplastic lesions. All the intestinal-type IPMNs concurrent with gastric-type IPMNs ( $n = 18$ ) or incipient PanIN-like lesions ( $n = 7$ ) shared identical *KRAS* and *GNAS* profiles with the gastric-type epithelia (Supplementary Tables S1 and S2). Intestinal-type IPMNs seemed to arise from gastric-type IPMNs with both *KRAS* and *GNAS* mutations ( $n = 14$ , 78%) or those with *GNAS* mutations only ( $n = 4$ , 22%). Furthermore, intestinal-type IPMNs seemed to arise from PanIN-like lesions, namely incipient IPMNs, with both *KRAS* and *GNAS* mutations ( $n = 4$ , 57%), and those with *GNAS* mutations only ( $n = 3$ , 43%). In fact, all the 25 intestinal-type IPMNs analyzed harbored *GNAS* mutations.

We evaluated the variant allele frequencies (VAFs) of mutant *GNAS* and *KRAS* under estimation of the same neoplastic cellularity, more than 80%, in the examined microdissected tissues. VAFs of *GNAS* and *KRAS* increased with the transition from gastric-type IPMNs into intestinal-type IPMNs as follows: VAFs of *GNAS* in gastric-type IPMNs and intestinal-type IPMNs were  $20.8 \pm 15.3\%$  and  $40.2 \pm 18.4\%$  ( $n = 18$ ,  $p = 0.00156$ , Supplementary Table S1 and Supplementary Fig. S7B), respectively. VAFs of *KRAS* in gastric-type IPMNs and intestinal-type IPMNs were  $23.1 \pm 12.1\%$  and  $33.8 \pm 12.4\%$  ( $n = 14$ ,  $p = 0.0284$ , Supplementary Table S1 and Supplementary Fig. S7A), respectively. Greater than or equal

**Fig. 4** Expression pattern of p21 and Ki-67 in intestinal IPMNs. HE staining and double immunostaining for p21 (nuclear red staining) and Ki-67 (nuclear green staining) in intestinal-type intraductal papillary mucinous neoplasms: low-grade dysplasia (b and f), high-grade dysplasia (c and g), invasive carcinoma (d and h), and a concurrent gastric-type component (a and e). Expression of p21 and Ki-67 seemed to be accelerated by CDX2 expression (e versus f or g). p21-positive cells mostly distribute in the apex, while Ki-67-positive cells do so in the base of papillae (f), which resembles normal intestinal mucosa (f, inset). Ki-67/p21 labeling index ratio (i) increased with malignant progression (one-way ANOVA,  $p = 0.00197$ , paired  $t$  test, low-grade intestinal-type IPMN versus high-grade intestinal-type IPMN,  $*p = 0.005$ , and versus invasive cancer,  $**p = 0.013$ ). Scatter plots are showing the distribution of p21 and Ki-67 labeling index according to tumor grades (j, k, and l). Labeling index of p21 tended to be higher than that of Ki-67 in intestinal-type IPMNs with low-grade dysplasia, but this trend was reversed with malignant progression. Phospho-PKA substrate Histo-score (m) increased in intestinal-type IPMNs (paired  $t$  test,  $p = 4.11e-06$ ). Phospho-ERK1/2 labeling index (n) increased in intestinal-type IPMNs (paired  $t$  test,  $p = 0.00291$ ). Scatter plot shows relationship of phospho-PKA substrate and phospho-ERK1/2 ( $r = 0.166$ , 95% CI  $-0.254-0.534$ ,  $p = 0.437$ ). LG, low-grade dysplasia; HG, high-grade dysplasia; INV, invasive cancer



to 2.0-fold increase of VAFs was observed in 9 IPMNs for *GNAS* (2.2–60.7-fold increase) and 5 IPMNs for *KRAS* (2.0–3.4-fold increase). Some intestinal-type IPMNs seemed to harbor *GNAS* mutations with loss of heterozygosity or

amplification because their VAFs were over 50%. Moreover, VAFs of *GNAS* and *KRAS* escalated during the transition from gastric-type incipient IPMN foci ( $7.5 \pm 6.9\%$  and  $3.5 \pm 3.7\%$ ) to mature intestinal-type IPMNs with papillary growth (47.1

$\pm 16.1\%$  and  $42.8 \pm 13.0\%$ ,  $n = 7$  and  $n = 3$ ,  $p = 0.000102$  and  $p = 0.0702$ , respectively, Supplementary Table S2 and Fig. 3o).

### Mutation and immunohistochemical analysis of tumor suppressor molecules in intestinal-type IPMNs

We examined mutations of *RNF43*, *CTNNB1*, *TP53*, *CDKN2A*, and *SMAD4* by means of targeted amplicon sequencing in 14 intestinal-type IPMNs and protein expressions of  $\beta$ -catenin, p53, p16, and SMAD4 in 25 IPMNs. *RNF43* mutations were frequently observed, i.e., 9 (64%) of the 14 cases harbored mutations (Supplementary Table S1). Among them, 10 mutations including 2 compound mutations were found in 8 of 14 intestinal-type components (57%), in which 5 mutations were newly emerged in the intestinal-type components compared with concurrent gastric-type components. Moreover, the remaining 5 mutations showed increasing of VAF in intestinal-type components compared with concurrent gastric-type components. All nonsense and missense *RNF43* mutations were considered pathogenic based on COSMIC (<https://cancer.sanger.ac.uk/cosmic>), ClinVar (<https://www.ncbi.nlm.nih.gov/clinvar/>), and/or SIFT/PROVEAN (<http://provean.jcvi.org/>).

Four *TP53* mutations were detected in 3 of the 14 intestinal-type IPMNs (21%) and 1 *CDKN2A* splice site mutation in 1 intestinal-type IPMNs (7%), and none was detected in concurrent gastric-type components. *RNF43* mutation was not detected in those 4 IPMNs harboring *TP53* or *CDKN2A* mutations. No *CTNNB1* and *SMAD4* mutation was detected in our cohort. Aberrant protein expression of  $\beta$ -catenin, p53, p16, and SMAD4 was observed in 20 cases (80%), 4 (16%), 12 (48%), and 0 (0%), respectively (Supplementary Table S1 and Table S2).

### Mechanism of induction of intrinsic CDX2 in intestinal-type IPMN

We performed immunohistochemical analysis for phospho-PKA substrate and phospho-ERK1/2 and evaluated their expression distinguishing the epithelial types in 25 IPMNs. Histo-score of phospho-PKA substrate was increased in intestinal-type IPMN ( $162.54 \pm 77.08$ ) than gastric type ( $59.05 \pm 45.08$ ) with statistical significance ( $p = 4.11 \times 10^{-6}$ , Fig. 4m). The labeling index of phospho-ERK1/2 was increased in intestinal-type IPMN ( $19.57 \pm 20.04\%$ ) than gastric type ( $4.25 \pm 8.92\%$ ) with statistical significance ( $p = 0.00291$ , Fig. 4n). Expression of phospho-ERK1/2 was frequently observed in the transition site from gastric to intestinal type and base of papillae. Expression of phospho-PKA substrate and phospho-ERK1/2 seemed to gradually increase with CDX2 expression in some IPMNs (Supplementary Fig. S8), though

the correlation between phospho-PKA substrate and phospho-ERK1/2 was not evident in this cohort ( $r = 0.166$ , 95% CI  $-0.254$ – $0.534$ ,  $p = 0.437$ , Fig. 4o).

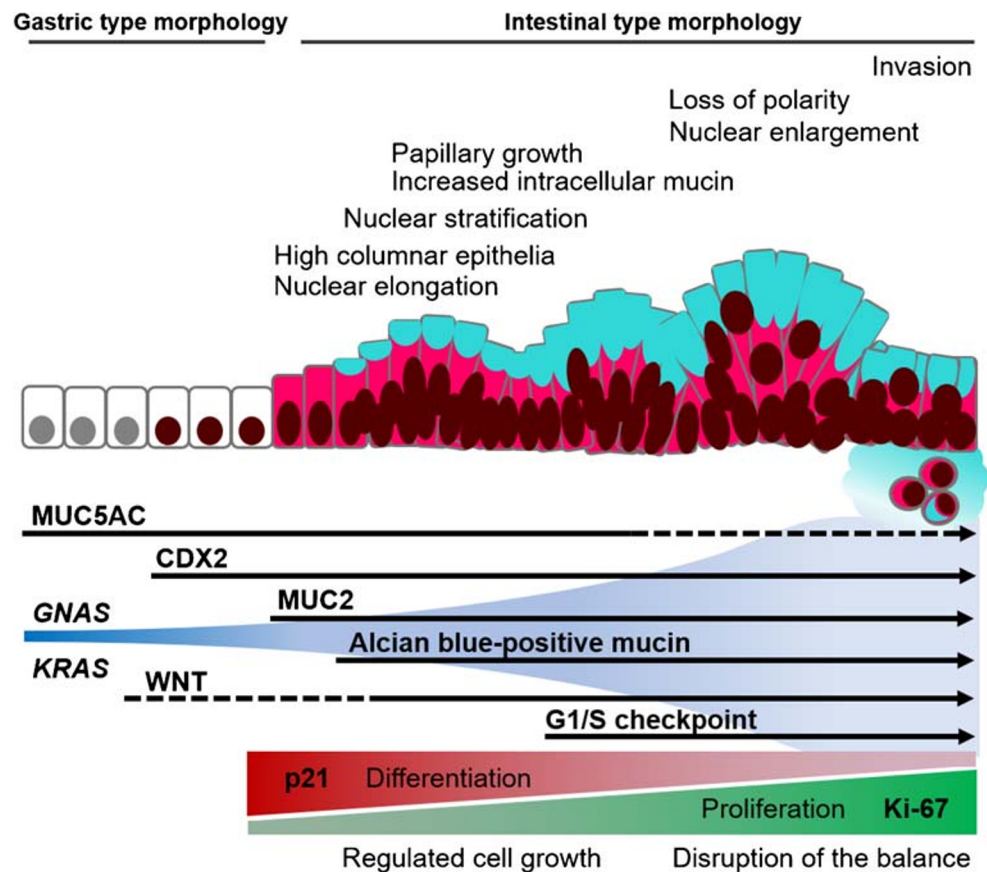
Expression of MLH1 was retained in all 60 IPMNs and microsatellite instability did not seem to be related with emergence of intestinal-type IPMN.

### Discussion

Tumorigenesis of IPMN is supposed to be initiated by gastric metaplasia-like change of pancreatic duct cells, which is indicated by common appearance of gastric foveolar features and MUC5AC expression in low-grade small IPMNs. Subsequent acquirement of intestinal features might be the diverging point in the development of intestinal-type IPMNs. Most of the intestinal IPMNs in our cohort involved the main duct and branch ducts. Most of the gastric-type components that showed transition resided in branch ducts. Besides, gastric-type IPMNs are known to involve preferentially branch ducts [4]. These observations suggest that intestinal-type IPMN may emerge from branch ducts and progress into the main duct. Previously, the appearance of CDX2-positive neoplastic cells in IPMNs coincided with that of MUC2-positive neoplastic cells was revealed by double immunostaining [15]. Our observation of CDX2 expression in gastric-type cells without obvious intestinal phenotypes strongly suggests that CDX2 may precede MUC2 expression and maturation of intestinal features, such as secretion of alcian blue-positive mucin in the neoplastic cells. We also observed that intestinal morphological features became obvious with MUC2 expression and that cytoplasmic mucin and papillary growth appeared more prominent as MUC2 expression increased. These results suggest that CDX2 may drive the characteristic biochemical and morphological transition of the gastric-type neoplastic component into the intestinal-type neoplastic component while promoting the expression of MUC2.

We also observed that CDX2 seemed to accelerate the expression of both p21 and Ki-67 in intestinal-type IPMNs. Interestingly, it has been reported that p21 is a transcriptional target of CDX2, a likely reason for the acceleration of p21 expression in the intestinal-type IPMNs [16]. On the other hand, the obvious increase of Ki-67-positive cell count suggests that CDX2 may induce some proliferation-promoting molecules in the intestinal-type IPMNs [10]. In our study, double immunostaining for p21 and Ki-67 revealed that the distribution of cells with p21 or Ki-67 in low-grade intestinal-type IPMNs was reminiscent of that in normal intestinal mucosa and colorectal serrated adenoma [17, 18], where the p21-positive cells resided mostly in the apex of papillae, an assumed differentiation zone, while the Ki-67-positive cells did so mostly in the base of papillae, an assumed proliferative zone. This suggests that the regulation mechanism of

**Fig. 5** Histologic and molecular progression model for intestinal-type intraductal papillary mucinous neoplasms



proliferation and differentiation for intestinal crypts may also be at work in the intestinal-type IPMNs, and this apparent regulation mechanism seems specific for the intestinal-type IPMNs compared with IPMNs of other subtypes. Hence, intestinal-type IPMNs may have a unique adenomatous phase with low-grade dysplasia, in which the balance of differentiation in p21-positive cells, and proliferation in Ki-67-positive cells, is regulated.

Furthermore, this regulated trend seemed to break down with the progression of grade and development of invasion, which is also observed in the process of colorectal tumorigenesis [18, 19]. RNF43 is an E3 ubiquitin ligase that acts as a WNT inhibitor by targeting WNT receptors for degradation. RNF43 is mutated and may play as a regulator of the DNA damage response in the sessile serrated neoplasia pathway of the colon, familial, and sporadic [20, 21]. RNF43 mutations are found in 23% of IPMNs [22]. In our cohort, 10 RNF43 mutations including 4 nonsense mutations, 3 missense mutations, and 3 frameshift mutations were detected in 8 (57%) of 14 intestinal-type IPMNs. Most of these RNF43 mutations were observed as intestinal-type specific emergence or accompanied by increase of VAF in existing mutations that were presumably due to loss of wild-type allele. These mutation phenotypes suggest that loss of function mutations in RNF43 may also play a driver role for the progression of the

gastric-type neoplasm into the intestinal-type neoplasm. The aberrant expression of  $\beta$ -catenin was observed in 80% of intestinal IPMNs with or without RNF43 mutation. Moreover, in the 14 intestinal-type IPMNs, 4 TP53 missense mutations were observed in 3 (21%) cases, 1 CDKN2A splice site mutation was observed in 1 case (7%), and aberrant protein expressions of p53 and p16 were observed in 16% and 48%, respectively (Supplementary Table S1 and Table S2). Hence, aberrations of the WNT signaling pathway by alteration of RNF43 and other signaling molecules or those of cell cycle checkpoints and apoptosis by TP53 and CDKN2A alterations may play an important role in dysregulation of p21 and Ki-67 expression and malignant progression in intestinal-type IPMNs. Intestinal-type IPMNs of the pancreas seemed to pursue intestinal-type tumorigenesis that involves aberrations of multiple signaling pathways [23, 24].

In our study, all of the 25 examined intestinal-type IPMNs remained genetically the same as the GNAS mutant gastric-type epithelium, regardless of grossly evident IPMNs or incipient lesions in size (Supplementary Table S1 and Table S2). Activating GNAS mutations are suggested crucial in intestinal-type IPMNs. However, at least in genetically engineered mouse models, the presence of GNAS mutation alone does not seem to induce the emergence of intestinal features [25–27]. RNF43 mutations are significantly

associated with *GNAS* mutations in IPMNs and are more frequently detected in intestinal-type IPMNs than non-intestinal types, even though statistically not significant [28]. We revealed that PKA substrate and ERK1/2 were activated in some intestinal-type IPMNs. The *GNAS* gene encodes the Gs $\alpha$  protein. The activated Gs $\alpha$  transmits a stimulating signal to an effector, adenylyl cyclase, which produces cyclic adenosine monophosphate (cAMP). cAMP binds to cAMP-dependent protein kinase A, thereby activating protein kinase A and the downstream signaling cascades, including ERK1/2 [29–31]. Intrinsic CDX2 might be induced by activation of the PKA/ERK axis in *GNAS* mutant intestinal IPMNs.

Among the morphologically and immunohistochemically similar neoplastic cells of low grade, only a portion of the cells seemed to harbor *GNAS* and *KRAS* mutations according to their variant allele frequencies (Supplementary Tables S1 and S2). The number of cells with mutation seemed to increase along with the phenotypic change from gastric to intestinal, reaching nearly hundred percent in high-grade neoplasia (Fig. 3o and Supplementary Fig. S7). The increase ratio exceeded 2.0-fold in several cases, and some intestinal-type IPMNs seemed to harbor *GNAS* mutations with loss of heterozygosity or amplification, as their VAFs were over 50%. These results suggest a clonal selection of cells with mutations during the progression from low-grade gastric-type neoplasms to high-grade intestinal-type neoplasms.

Based on the results of our study, we propose a model for the progression of gastric-type IPMNs into intestinal-type IPMNs with emphasis on the timing of acquisition of intestinal features apparently driven by CDX2, the clonal evolution of *GNAS* mutant cells, acquisition and selection of *RNF43* mutations, and the breakdown of cell cycle regulation during the maturation of intestinal phenotype, progression of dysplastic grade, and development of invasion (Fig. 5). Mutant *GNAS* may induce CDX2 expression in conjunction with some other molecules, e.g., *RNF43* and activation of PKA and ERK1/2, that might depend on certain yet unknown microenvironmental factors. How CDX2 is induced in *GNAS* mutant gastric-type neoplasms remains a significant question for future research.

**Acknowledgments** We would like to thank Ms. Fumiko Date (Biomedical Research Core of Tohoku University Graduate School of Medicine) for tissue sample preparation, and Ms. Yuko Hayakawa (Sapporo Higashi Tokushukai Hospital) for technical support in the genetic analysis. The authors would also like to thank Mr. David Hochman for the editorial review of the manuscript.

**Author's contributions** Y. Omori and T.F. performed the histological analysis; Y. Omori performed the immunohistochemical analysis; Y. Omori and Y. Ono performed genetic analysis and Y. Omori interpreted the data; T.K., F.M., and M.U. collected clinical samples; Y. Omori obtained the funding; Y.M., H.K., N.M., Y.U., and T.F. supervised the project; Y. Omori developed the concept, designed experimental studies, analyzed the data, and wrote the manuscript with feedback from all

authors. T.F. is the guarantor of this work and, as such, had full access to all of the data in the study and takes responsibility for the integrity of the data and the accuracy of the data analysis.

**Funding information** This work was supported by the Japan Society for the Promotion of Science, KAKENHI Grant Number JP19K16576 (to Y. Omori).

**Data availability** Supplementary information is available at Virchows Arch's website.

## Compliance with ethical standards

This study was approved by the Institutional Review Board of Tohoku University, Graduated School of Medicine (#2018-1-752).

**Conflict of interests** The authors declare that they have no conflicts of interest.

## References

1. Furukawa T, Klöppel G, Volkan Adsay N, Albores-Saavedra J, Fukushima N, Horii A, Hruban RH, Kato Y, Klimstra DS, Longnecker DS, Lüttges J, Offerhaus GJ, Shimizu M, Sunamura M, Suriawinata A, Takaori K, Yonezawa S (2005) Classification of types of intraductal papillary-mucinous neoplasm of the pancreas: a consensus study. *Virchows Arch* 447:794–799
2. Adsay V, Mino-Kenudson M, Furukawa T, Basturk O, Zamboni G, Marchegiani G, Bassi C, Salvia R, Malleo G, Paiella S, Wolfgang CL, Matthaei H, Offerhaus GJ, Adham M, Bruno MJ, Reid MD, Krasinskas A, Klöppel G, Ohike N, Tajiri T, Jang KT, Roa JC, Allen P, Fernández-del Castillo C, Jang JY, Klimstra DS, Hruban RH (2016) Pathologic evaluation and reporting of intraductal papillary mucinous neoplasms of the pancreas and other tumoral intraepithelial neoplasms of pancreatobiliary tract: recommendations of Verona consensus meeting. *Ann Surg* 263:162–177
3. Basturk O, Hong SM, Wood LD, Adsay NV, Albores-Saavedra J, Biankin AV, Brosens LA, Fukushima N, Goggins M, Hruban RH, Kato Y, Klimstra DS, Klöppel G, Krasinskas A, Longnecker DS, Matthaei H, Offerhaus GJ, Shimizu M, Takaori K, Terris B, Yachida S, Esposito I, Furukawa T (2015) A revised classification system and recommendations from the Baltimore consensus meeting for neoplastic precursor lesions in the pancreas. *Am J Surg Pathol* 39:1730–1741
4. Furukawa T, Hatori T, Fujita I, Yamamoto M, Kobayashi M, Ohike N, Morohoshi T, Egawa S, Unno M, Takao S, Osako M, Yonezawa S, Mino-Kenudson M, Lauwers GY, Yamaguchi H, Ban S, Shimizu M (2011) Prognostic relevance of morphological types of intraductal papillary mucinous neoplasms of the pancreas. *Gut* 60:509–516
5. Gum JR, Byrd JC, Hicks JW, Toribara NW, Lampion DT, Kim YS (1989) Molecular cloning of human intestinal mucin cDNAs. Sequence analysis and evidence for genetic polymorphism. *J Biol Chem* 264:6480–6487
6. Kwak HA, Liu X, Allende DS, Pai RK, Hart J, Xiao SY (2016) Interobserver variability in intraductal papillary mucinous neoplasm subtypes and application of their mucin immunoprofiles. *Mod Pathol* 29:977–984
7. Adsay NV, Merati K, Basturk O, Iacobuzio-Donahue C, Levi E, Cheng JD, Sarkar FH, Hruban RH, Klimstra DS (2004) Pathologically and biologically distinct types of epithelium in intraductal papillary mucinous neoplasms: delineation of an

- “intestinal” pathway of carcinogenesis in the pancreas. *Am J Surg Pathol* 28:839–848
8. Allen A, Hutton DA, Pearson JP (1998) The MUC2 gene product: a human intestinal mucin. *Int J Biochem Cell Biol* 30:797–801
  9. James R, Erler T, Kazenwadel J (1994) Structure of the murine homeobox gene *cdx2*. Expression in embryonic and adult intestinal epithelium. *J Biol Chem* 269:15229–15237
  10. Guo RJ, Suh ER, Lynch JP (2004) The role of Cdx proteins in intestinal development and cancer. *Cancer Biol Ther* 3:593–601
  11. Yamamoto H, Bai Y-Q, Yuasa Y (2003) Homeodomain protein CDX2 regulates goblet-specific MUC2 gene expression. *Biochem Biophys Res Commun* 300:813–818
  12. Kuboki Y, Shimizu K, Hatori T, Yamamoto M, Shibata N, Shiratori K, Furukawa T (2015) Molecular biomarkers for progression of intraductal papillary mucinous neoplasm of the pancreas. *Pancreas* 44:227–235
  13. Furukawa T, Fukushima N, Itoi T, Ohike N, Mitsuhashi T, Nakagohri T, Notohara K, Shimizu M, Tajiri T, Tanaka M, Yamaguchi H, Yanagisawa A, Sugiyama M, Okazaki K (2019) A consensus study of the grading and typing of intraductal papillary mucinous neoplasms of the pancreas. *Pancreas* 48:480–487
  14. Omori Y, Ono Y, Tanino M, Karasaki H, Yamaguchi H, Furukawa T, Enomoto K, Ueda J, Sumi A, Katayama J, Muraki M, Taniue K, Takahashi K, Ambo Y, Shinohara T, Nishihara H, Sasajima J, Maguchi H, Mizukami Y, Okumura T, Tanaka S (2019) Pathways of progression from intraductal papillary mucinous neoplasm to pancreatic ductal adenocarcinoma based on molecular features. *Gastroenterology* 156:647–661.e2
  15. Yeh TS, Ho YP, Chiu CT, Chen TC, Jan YY, Chen MF (2005) Aberrant expression of CDX2 homeobox gene in intraductal papillary-mucinous neoplasm of the pancreas but not in pancreatic ductal adenocarcinoma. *Pancreas* 30:233–238
  16. Bai YQ, Miyake S, Iwai T, Yuasa Y (2003) CDX2, a homeobox transcription factor, upregulates transcription of the p21/WAF1/CIP1 gene. *Oncogene* 22:7942–7949
  17. Jiao YF, Nakamura S, Sugai T, Yamada N, Habano W (2008) Serrated adenoma of the colorectum undergoes a proliferation versus differentiation process: new conceptual interpretation of morphogenesis. *Oncology* 74:127–134
  18. Komori K, Ajioka Y, Watanabe H, Oda K, Nimura Y (2003) p21<sup>WAF1/CIP1</sup> and Ki-67 expression of serrated adenoma of the colorectum: an investigation of cell differentiation/maturation and its relationship with cell proliferation. *Acta Med Biol* 51:117–124
  19. Doglioni C, Pelosio P, Laurino L, Macri E, Meggiolaro E, Favretti F, Barbareschi M (1996) p21/WAF1/CIP1 expression in normal mucosa and in adenomas and adenocarcinomas of the colon: its relationship with differentiation. *J Pathol* 179:248–253
  20. Gala MK, Mizukami Y, Le LP, Moriichi K, Austin T, Yamamoto M, Lauwers GY, Bardeesy N, Chung DC (2014) Germline mutations in oncogene-induced senescence pathways are associated with multiple sessile serrated adenomas. *Gastroenterology* 146:520–529
  21. Yan HHN, Lai JCW, Ho SL, Leung WK, Law WL, Lee JFY, Chan AKW, Tsui WY, Chan ASY, Lee BCH, Yue SSK, Man AHY, Clevers H, Yuen ST, Leung SY (2017) RNF43 germline and somatic mutation in serrated neoplasia pathway and its association with BRAF mutation. *Gut* 66:1645–1656
  22. Lee JH, Kim Y, Choi JW, Kim YS (2016) KRAS, GNAS, and RNF43 mutations in intraductal papillary mucinous neoplasm of the pancreas: a meta-analysis. *Springerplus* 26:1172
  23. Kinzler KW, Vogelstein B (1996) Lessons from hereditary colorectal cancer. *Cell* 18:159–170
  24. Network CGA (2012) Comprehensive molecular characterization of human colon and rectal cancer. *Nature* 487:330–337
  25. Taki K, Ohmuraya M, Tanji E, Komatsu H, Hashimoto D, Semba K, Araki K, Kawaguchi Y, Baba H, Furukawa T (2016) GNAS<sup>R201H</sup> and Kras<sup>G12D</sup> cooperate to promote murine pancreatic tumorigenesis recapitulating human intraductal papillary mucinous neoplasm. *Oncogene* 35:2407–2412
  26. Patra KC, Kato Y, Mizukami Y, Widholz S, Boukhali M, Revenco I, Grossman EA, Ji F, Sadreyev RI, Liss AS, Sreanor RA, Sakamoto K, Ryan DP, Mino-Kenudson M, Castillo CF, Nomura DK, Haas W, Bardeesy N (2018) Mutant GNAS drives pancreatic tumorigenesis by inducing PKA-mediated SIK suppression and reprogramming lipid metabolism. *Nat Cell Biol* 20:811–822
  27. Ideno N, Yamaguchi H, Ghosh B, Gupta S, Okumura T, Steffen DJ, Fisher CG, Wood LD, Singhi AD, Nakamura M, Gutkind JS, Maitra A (2018) GNAS<sup>R201C</sup> induces pancreatic cystic neoplasms in mice that express activated KRAS by inhibiting YAP1 signaling. *Gastroenterology* 155:1593–1607.e12
  28. Sakamoto H, Kuboki Y, Hatori T, Yamamoto M, Sugiyama M, Shibata N, Shimizu K, Shiratori K, Furukawa T (2015) Clinicopathological significance of somatic RNF43 mutation and aberrant expression of ring finger protein 43 in intraductal papillary mucinous neoplasms of the pancreas. *Mod Pathol* 28:261–267
  29. Dhanasekaran DN (2006) Transducing the signals: a G protein takes a new identity. *Sci STKE* 347:pe31
  30. Landis CA, Masters SB, Spada A, Pace AM, Bourne HR, Vallar L (1989) GTPase inhibiting mutations activate the alpha chain of Gs and stimulate adenylyl cyclase in human pituitary tumours. *Nature* 340:692–696
  31. Komatsu H, Tanji E, Sakata N, Aoki T, Motoi F, Naitoh T, Katayose Y, Egawa S, Unno M, Furukawa T (2014) A GNAS mutation found in pancreatic intraductal papillary mucinous neoplasms induces drastic alterations of gene expression profiles with upregulation of mucin genes. *PLoS One* 9:e87875

**Publisher's note** Springer Nature remains neutral with regard to jurisdictional claims in published maps and institutional affiliations.